Ceramics International 24 (1998) 61–66
© 1997 Elsevier Science Limited and Techna S.r.l.
Printed in Great Britain. All rights reserved
0272-8842/97 $17.00+.00
PII: S0272-8842(96)00080-6

Superplasticity in Al_2O_3–20 vol% Spinel ($MgO \cdot 1{\cdot}5Al_2O_3$) Ceramics

Y. Takigawa,[a*] Y. Yoshizawa[b] & T. Sakuma[a]

[a]Department of Materials Science, Faculty of Engineering, The University of Tokyo, 7-3-1 Hongo, Bunkyo-ku, Tokyo 113, Japan
[b]Ceramic Science Department, National Industrial Research Institute of Nagoya, 1-1 Hirate-cho, Kita-ku, Nagoya 462, Japan

(Received 3 June 1996; accepted 15 July 1996)

Abstract: Superplasticity in Al_2O_3–20 vol% spinel ($MgO \cdot 1{\cdot}5Al_2O_3$) is investigated by means of tensile testing in the temperature range 1300–1550°C. The dispersion of spinel phase in Al_2O_3 slightly reduces the flow stress, and highly enhances the high-temperature ductility at the same stress level in comparison with 0·1 wt% MgO-doped single-phase Al_2O_3. A maximum elongation of 396% is obtained at 1550°C and a strain rate of $2{\cdot}4 \times 10^{-4} s^{-1}$. The flow stress reduction is associated with a slight reduction in activation energy for superplastic flow. The extensive ductility in Al_2O_3–20 vol% spinel cannot be explained only from the stress reduction. The Al_2O_3/spinel boundaries are expected to have much larger resistance to crack extension than Al_2O_3 grain boundaries.

1 INTRODUCTION

Superplasticity in ceramics has been widely studied in recent years.[1–18] Tensile elongation in excess of 100% is obtained in fine-grained ceramics whose grain size is less than about 1 μm. Among various fine-grained ceramics, yttria-stabilized tetragonal zirconia polycrystal (Y–TZP) exhibits huge elongation, up to 800%, at high temperatures.[17] The extensive ductility in Y–TZP is explained in terms of grain size stability during high temperature deformation.[19]

In contrast to Y–TZP, the tensile ductility of fine-grained Al_2O_3 is very limited; the elongation of high-purity Al_2O_3 with a grain size of 0·90 μm is only 18% at 1400°C.[20] The limited ductility of Al_2O_3 arises from extensive grain growth and resultant cavitation during high-temperature plastic flow.[20] A small addition of MgO into high-purity Al_2O_3 inhibits the concurrent grain growth during deformation, and hence improves the tensile ductility.[16,20–26] In 0·1 wt% MgO-doped single-phase Al_2O_3, an elongation of over 100% is obtained in temperature-raising tests, which are effective in suppressing grain growth during deformation.[16]

The present paper aims to report the improvement of tensile ductility of Al_2O_3 due to the dispersion of spinel ($MgO \cdot 1{\cdot}5Al_2O_3$) phase and to discuss the origin of the ductility improvement.

2 EXPERIMENTAL

High-purity alumina powders of 99·99% purity, with an average diameter of 0·2 μm, supplied by Taimei Chemical Co. Ltd (TM-DAR) and high-purity magnesia powders of 99·97% purity, with about 17 nm diameter, supplied by Ube Co. Ltd were used for starting materials. Al_2O_3–20 vol% - spinel was prepared from these powders as follows. They were mixed in a ball mill in ethanol, together with 5 mm diameter high-purity alumina balls, for 24 h, and then dried and sifted through a 60 mesh sieve for granulation. The sifted powders were pressed under a pressure of 33 MPa, and further cold-isostatically pressed under a pressure of 100 MPa in a rubber tube. Sintering was carried out at 1400°C for 2 h in air. The bulk density of the

Research Fellow of the Japan Society for the Promotion of Science (Graduate student, The University of Tokyo).

sintered bodies was measured using the Archimedes technique. Tensile test specimens were cut and ground from the sintered bodies. The specimen size was 2 mm×2 mm×13·5 mm in gauge length. Uniaxial tensile tests were carried out in the temperature range 1300–1550°C in air. An Instron-type mechanical testing machine Shimadzu AG-5000C, equipped with a high-temperature furnace and SiC tensile jigs, was used. XRD (X-ray diffraction) studies were carried out with Mac Science MXP-18. The microstructure was examined with a scanning electron microscope (SEM) JEOL JSM-5200. For SEM examinations, ground and polished samples were thermally-etched at a temperature of about 50°C below the sintering or testing temperatures, and further chemically etched in a mixture of concentrated sulphuric acid and orthophosphoric acid (3:1 by volume) at 200°C for 10 min. They were coated with gold film using an ion spattering machine. The grain size was measured with linear intercept method on SEM photographs.

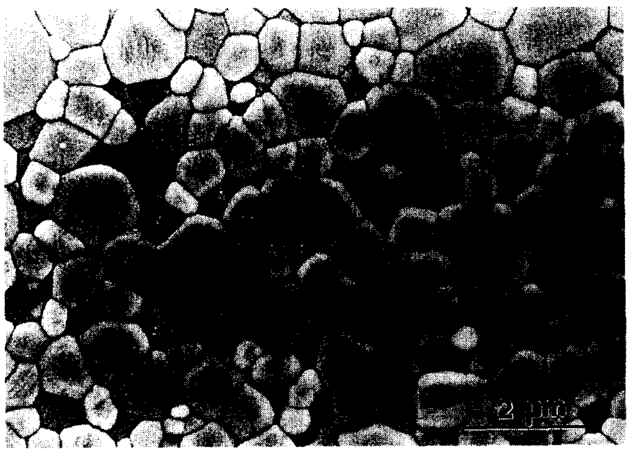

Fig. 1. Scanning electron micrograph of Al_2O_3–20 vol% spinel sintered at 1400°C for 2 h. "A" and "S" represent Al_2O_3 and spinel grains, respectively.

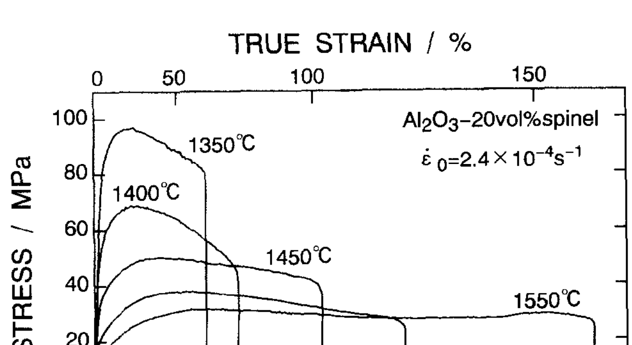

Fig. 2. Stress–strain curves in Al_2O_3–20 vol% spinel deformed at a temperature between 1350 and 1550°C and an initial strain rate of $2{\cdot}4\times10^{-4}\,s^{-1}$.

3 RESULTS

Figure 1 shows the scanning electron micrograph of as-sintered Al_2O_3–20 vol% spinel. The relative density is about 99% and the average grain size is 1·1 μm in the as-sintered state. In the micrograph, the grains with light grey contrast are Al_2O_3 and those with dark gray contrast are spinel. Some Al_2O_3 and spinel grains are marked as "A" and "S", respectively, in Fig. 1. From XRD studies, the ratio of Al_2O_3 and MgO in spinel is estimated to be 1·47 at 1400°C and 1·64 at 1500°C, which is in good agreement with the previous report.[27]

The stress–strain curves in Al_2O_3–20 vol% spinel deformed at various temperatures are shown in Fig. 2. In the temperature range examined, the flow stress decreases and the elongation to failure increases with an increase of temperature. A maximum elongation of 396% is obtained at 1550°C, which is probably the largest elongation in Al_2O_3-based ceramics reported so far. The photograph of the sample which failed at 1550°C is shown in Fig. 3. The specimen is deformed almost uniformly throughout the specimen gauge and necking is not observed as well as other superplastic ceramics.[13]

Figure 4 is a comparison of the stress–strain curves between Al_2O_3–20 vol% spinel and 0·1 wt% MgO-doped single-phase Al_2O_3, whose initial grain size is 0·8 μm.[16] It is interesting to note that Al_2O_3–20 vol% spinel has a higher peak stress than 0·1 wt% MgO-doped Al_2O_3 at each temperature, but the tensile ductility is very much improved by spinel dispersion.

Figure 5 is a plot of log 10% flow stress against log strain rate. The strain rate sensitivity value of *m* (estimated from strain rate change tests) is about 0·6, except at low strain rates below about $2\times10^{-5}\,s^{-1}$. The *m* value is close to that obtained from the slope of the straight line at each temperature in Fig. 5.

A log–log plot of 5% flow stress against grain size in 0·1 wt% MgO-doped Al_2O_3 and Al_2O_3–20 vol% spinel is shown in Fig. 6. The relationship

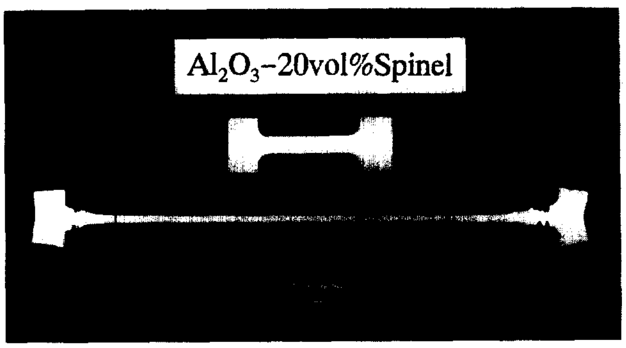

Fig. 3. Photograph of Al_2O_3–20 vol% spinel undeformed (upper) and failed at 396% strain at 1550°C (lower).

is approximated to be a straight line in each material, but the flow stress at the same grain size is reduced by spinel dispersion. The slope of the straight lines, which is equal to a product of *m* and grain size exponent *p*, is calculated to be 1·8 in the two materials. In 0·1 wt% MgO-doped Al_2O_3, *m* is reported to be about 0·6,[16] as well as in Al_2O_3–20 vol% spinel, and hence the grain size exponent *p* becomes about 3 in both materials.

Figure 7 is a plot of log strain rate (at a flow stress of 60 MPa) against inverse temperature in Al_2O_3–20 vol% spinel. From the slope of the straight line, the activation energy is estimated to be 364 kJ/mol.

Figure 8 is the grain size change with strain in Al_2O_3–20 vol% spinel, together with the previous data on pure Al_2O_3 and 0·1 wt% MgO-doped Al_2O_3.[20] The grain growth in Al_2O_3–20 vol% spinel is much more sluggish than that in pure Al_2O_3, but is not so different from that in 0·1 wt% MgO-doped Al_2O_3.

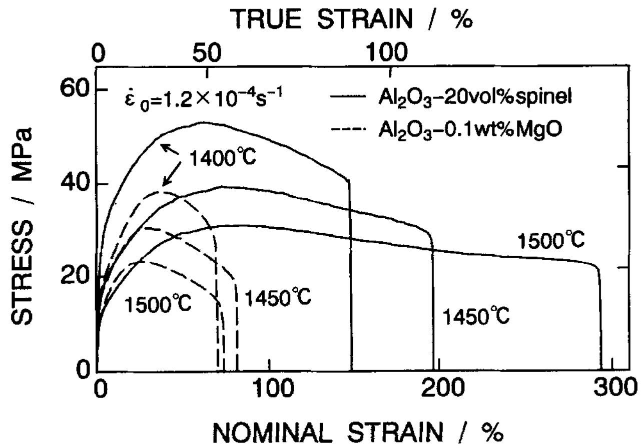

Fig. 4. The stress–strain curves in 0·1 wt% MgO-doped Al_2O_3[16] and Al_2O_3–20 vol% spinel for an initial strain rate of $1{\cdot}2\times10^{-4}\,s^{-1}$.

4 DISCUSSION

The strain rate ($\dot{\varepsilon}$) vs stress (σ) relationship in superplastic ceramics has been discussed from the following semiempirical equation:

$$\dot{\varepsilon} = A\frac{\sigma^n}{d^p}\exp\left(-\frac{Q}{RT}\right) \qquad (1)$$

where *A* is the constant depending on the microstructure and deformation mechanism, *n* is the stress exponent, which is the inverse strain rate sensitivity *m*, *p* is the grain size exponent, *Q* is the activation energy and *RT* is the gas constant times absolute temperature.

The *m* and *p* values obtained in Al_2O_3–20 vol% -spinel are almost the same as those in 0·1 wt% MgO-doped Al_2O_3, i.e. *m* is about 0·6 and *p* is about 3 in both materials, as described before. However, as shown in Fig. 6, the flow stress–grain size relationship is different between the two materials. The flow stress in Al_2O_3–20 vol% spinel is lower than that in 0·1 wt% MgO-doped Al_2O_3 at the same grain size. The difference may be caused by the difference in activation energy *Q*. The activation energy is not reported in 0·1 wt% MgO-doped Al_2O_3, but the value can be roughly estimated to be about 400 kJ/mol from the reported stress–strain rate relationship.[16] This value is not so different from the value of 419 kJ/mol for the activation energy for grain boundary diffusion of Al^{3+} in Al_2O_3 reported by Cannon *et al.*[22] The activation energy of 364 kJ/mol in Al_2O_3–20 vol% spinel obtained in this study is a little smaller than that in 0·1 wt% MgO-doped Al_2O_3. The slight reduction in activation energy due to spinel dispersion in Al_2O_3 must be a major origin of the decrease in flow stress at the same grain size level in comparison with 0·1 wt% MgO-doped Al_2O_3, as shown in Fig. 6, although the diffusion

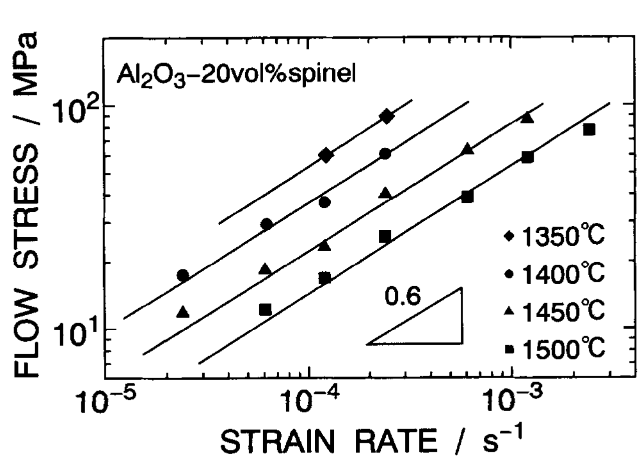

Fig. 5. A log–log plot of 10% flow stress against strain rate in Al_2O_3–20 vol% spinel.

species and path controlling the superplastic flow cannot be identified because of the limited diffusivity data. The situation is similar to the enhanced superplastic flow in TZP with TiO_2 doping.[28]

Another important fact clarified in this study is that the large elongation in Al_2O_3–20 vol% spinel is not simply related to the flow stress reduction. Figure 9 is a plot of fracture strain against log(peak stress) in Al_2O_3–20 vol% spinel, together with the previous data on 0·1 wt% MgO-doped Al_2O_3 and Al_2O_3–10 wt% ZrO_2.[29] The relationship is represented by a single straight line in 0·1 wt% MgO-doped Al_2O_3 and Al_2O_3–10 wt% ZrO_2. The limited ductility in Al_2O_3–10 wt% ZrO_2 is explained in terms of flow stress increment with ZrO_2 addition.[29] In contrast to Al_2O_3–10 wt% ZrO_2, the fracture strain–peak stress relationship in Al_2O_3–20 vol% spinel is very different from that in the other two materials. The fracture strain at the same stress level is very large in Al_2O_3–20 vol% spinel, in comparison with 0·1 wt% MgO-doped Al_2O_3 or Al_2O_3–10 wt% ZrO_2.

Figure 10 shows the optical micrographs of 0·1 wt% MgO-doped Al_2O_3 and Al_2O_3–20 vol% spinel, deformed by 50% at 1450°C and an initial strain rate of $1{\cdot}2\times10^{-4}\,s^{-1}$. In 0·1 wt% MgO-doped Al_2O_3, many crack-like cavities are developed normal to the tensile axis, while no large crack-like cavities are formed and only small cavities generate in Al_2O_3–20 vol% spinel. The crack-like cavity growth is very limited in Al_2O_3–20 vol% spinel. In Al_2O_3–20 vol% spinel, there are three types of boundaries, i.e. Al_2O_3/Al_2O_3 boundaries, Al_2O_3/spinel boundaries and spinel/spinel boundaries.

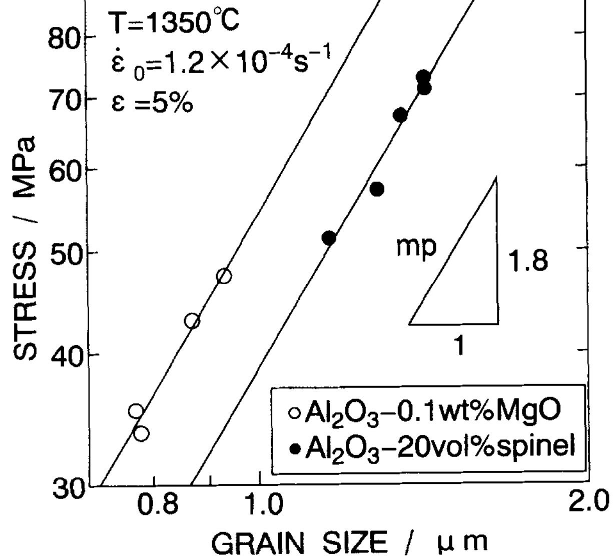

Fig. 6. The relationship between grain size and 5% flow stress at 1350°C and a strain rate of $1{\cdot}2\times10^{-4}\,s^{-1}$.

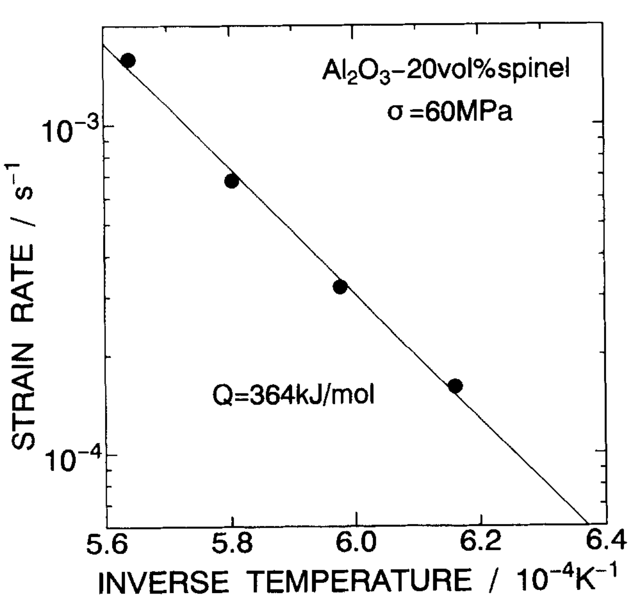

Fig. 7. The strain rate at a stress of 60 MPa as a function of inverse temperature in Al_2O_3–20 vol% spinel.

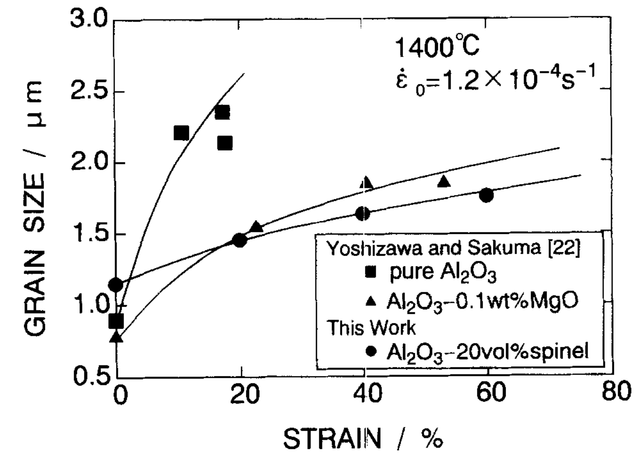

Fig. 8. Grain size change of pure Al_2O_3, 0·1 wt% MgO-doped Al_2O_3 and Al_2O_3–20 vol% spinel as a function of strain.

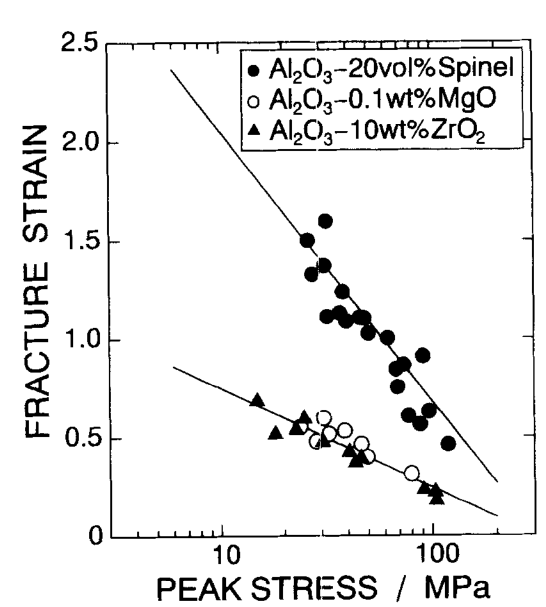

Fig. 9. The relationship between fracture strain and peak stress in Al_2O_3–10 wt% ZrO_2,[29] Al_2O_3–20 vol% spinel and 0·1 wt% MgO-doped Al_2O_3.

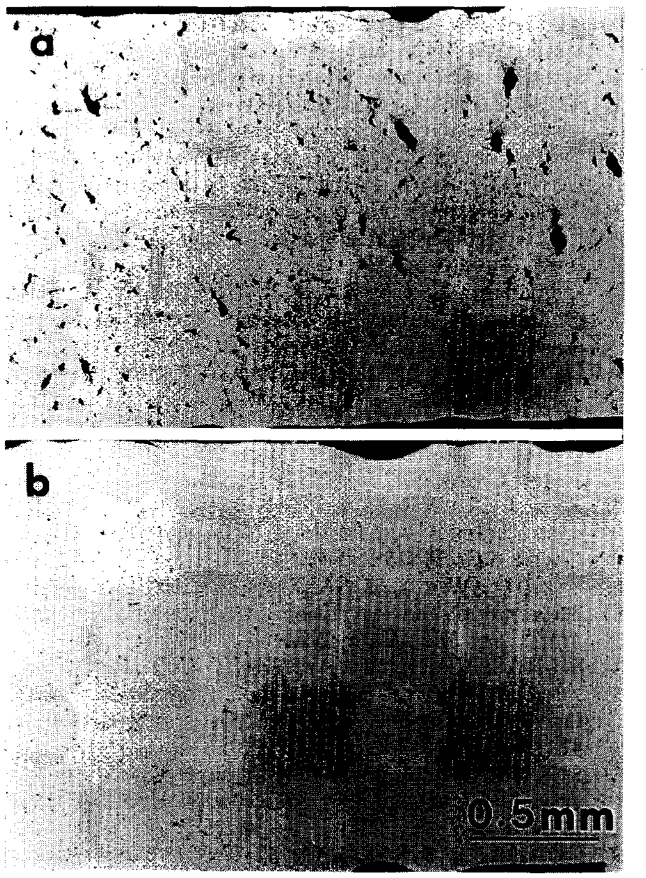

Fig. 10. Optical micrographs of 50% deformed samples in (a) 0·1 wt% MgO-doped Al_2O_3 and (b) Al_2O_3–20 vol% spinel at 1450°C and an initial strain rate of $1{\cdot}2\times10^{-4}\,s^{-1}$. The tensile direction is horizontal.

Since the fraction of spinel/spinel boundaries is small in Al_2O_3–20 vol% spinel, the limited cavity growth may be caused by the presence of Al_2O_3/spinel boundaries. Namely, it is possible to expect that the crack extension is suppressed along Al_2O_3/spinel boundaries in comparison with Al_2O_3/Al_2O_3 boundaries. The resistance to crack extension along Al_2O_3/spinel boundaries may be associated with the non-stoichiometry of the spinel phase, as pointed out by Lappalainen *et al.*[30] More details on crack extension in Al_2O_3–20 vol% spinel are reported elsewhere.

5 CONCLUSION

Superplastic flow in Al_2O_3–20 vol% spinel is examined. The results obtained are summarized as follows:

(a) The dispersion of the spinel phase is very effective in improving the tensile ductility of Al_2O_3 at high temperatures, and a maximum elongation of about 400% is obtained at 1550°C and an initial strain rate of $2{\cdot}4\times10^{-4}\,s^{-1}$.

(b) The flow stress at the same grain size is reduced by spinel dispersion in Al_2O_3. This is likely to be caused by a slight reduction in activation energy for superplastic flow.

(c) The extensive ductility in Al_2O_3–20 vol%-spinel can not simply be explained from the flow stress reduction due to the presence of spinel phase, because the fracture strain–peak stress relationship is very different between 0·1 wt% MgO-doped Al_2O_3 and Al_2O_3–20 vol% spinel. Crack expansion must be more effectively suppressed along Al_2O_3/spinel boundaries than along Al_2O_3/Al_2O_3 boundaries.

ACKNOWLEDGEMENTS

The authors express their gratitude for the financial support of the Grant-in-Aid for Scientific Research on the priority Area "Innovation in Superplasticity" (08242103) and for Developmental Scientific Research (06555202) from the Ministry of Education, Science and Culture, Japan.

REFERENCES

1. WAKAI, F., SAKAGUCHI, S. & MATSUNO, Y., Superplasticity of yttria-stabilized tetragonal ZrO_2 polycrystals. *Adv. Ceram. Mater.*, **1** (1986) 259–263.
2. MAEHARA, Y. & LANGDON, T. G., Review: Superplasticity in ceramics. *J. Mater. Sci.*, **25** (1990) 2275–2286.
3. LANGDON, T. G., Superplastic ceramic — an overview. In *Superplasticity in Aerospace II*, ed. T. R. McNelley & H. C. Heikkenen. TMS, Warrendale, PA, 1990, pp. 3–18.
4. CHEN, I.-W. & XUE, L. A., Development of superplastic structural ceramics. *J. Am. Ceram. Soc.*, **73** (1990) 2585–2609.
5. SAKUMA, T., Micrograin superplasticity in ceramics. In *Proc. 1st Pacific Rim Int. Conf. on Advanced Materials and Processing*, ed. C. Shi, H. Li & A. Scott. TMS, Warrendale, PA, 1992, pp. 881–886.
6. MUKHERJEE A. K., Superplasticity in metals, ceramics and intermetallics. In *Material Science and Technology, Vol. 6: Plastic Deformation and Fracture of Materials*, ed. H. Mughrabi. VCH, Weinheim, 1993, p. 407.
7. WADSWORTH, J. & NIEH, T. G., Superplasticity in ceramics and metal matrix composites and the role of grain size, segregation, interface and second phase morphology. *Mater. Sci. Eng.*, **A166** (1993) 97–108.
8. CHOKSHI, A. H., Superplasticity in fine grained ceramics and ceramic composites: Current understanding and future prospects. *Mater. Sci. Eng.*, **A166** (1993) 119–133.
9. CHOKSHI, A. H., MUKHERJEE, A. K. & LANGDON, T. G., Superplasticity in advanced materials. *Mater. Sci. Eng.*, **R10** (1993) 237–274.
10. NIEH, T. G. & WADSWORTH, J., Superplasticity in fine-grained 20% Al_2O_3/YTZ composite. *Acta Metall. Mater.*, **39** (1991) 3037–3045.

11. WAKAI, F., KODAMA, Y., SAKAGUCHI, S., MURAYAMA, N., IZAKI, K. & NIIHARA, K., A superplastic covalent crystal composite. *Nature*, **344** (1990) 421–423.
12. WAKAI, F., KODAMA, Y., SAKAGUCHI, S. & NONAMI, T., Superplasticity of hot isostatically pressed hydroxyapatite. *J. Am. Ceram. Soc.*, **73** (1990) 457–460.
13. KIM, W. J., WOLFENSTINE, J. & SHERBY, O. D., Tensile ductility of superplastic ceramics and metallic alloys. *Acta Metall. Mater.*, **39** (1991) 199–208.
14. WU, X. & CHEN, I.-W., Exaggerated texture and grain growth in a superplastic SiAlON. *J. Am. Ceram. Soc.*, **75** (1992) 2733–2741.
15. WANG, Z. C., DAVIES, T. J. & RIDLEY, N., Net shape fabrication of ceramic specimens for superplastic tensile testing. *Scripta Metall. Mater.*, **28** (1993) 301–306.
16. YOSHIZAWA, Y. & SAKUMA, T., High temperature deformation in fine grained alumina. In *Aspects of High Temperature Deformation and Fracture in Crystalline Materials*, ed. Y. Hosoi, H. Yoshinaga, H. Oikawa & K. Maruyama. The Japan Institute of Metals, Nagoya, 1993, pp. 463–469.
17. NIEH, T. G. & WADSWORTH, J., Superplastic behaviour of a fine-grained yttria-stabilized tetragonal zirconia polycrystal (Y–TZP). *Acta Metall. Mater.*, **38** (1990) 1121–1133.
18. KAJIHARA, K., YOSHIZAWA, Y. & SAKUMA, T., Superplasticity in SiO_2-containing tetragonal zirconia polycrystal. *Scripta Metall. Mater.*, **28** (1993) 559–562.
19. SAKUMA, T., YOSHIZAWA, Y. & OKADA, K., High-temperature plastic flow and cavitation in fine-grained ceramics. In *Creep and Fracture of Engineering Materials and Structures*, ed. B. Wilshire & R. E. Evans. The Institute of Materials, London, 1993, pp. 305–314.
20. YOSHIZAWA, Y. & SAKUMA, T., Improvement of tensile ductility in high-purity alumina due to magnesia addition. *Acta Metall. Mater.*, **40** (1992) 2943–2950.
21. YOSHIZAWA, Y. & SAKUMA, T., Grain growth acceleration during high temperature deformation in high purity alumina. *Mater. Sci. Eng.*, **A149** (1991) 59–64.
22. CANNON, R. M., RHODES, W. H. & HEUER, A. H., Plastic deformation of fine-grained alumina (Al_2O_3) — I. Interface-controlled diffusional creep. *J. Am. Ceram. Soc.*, **63** (1980) 46–53.
23. GRUFFEL, P., CARRY, P. & MOCELLIN, A., Effect of testing conditions on superplastic creep of alumina doped with Ti and Y. In *Science of Ceramics*, Vol. 14, ed. D. Taylor. The Institute of Ceramics, Shelton, Stoke-on-Trent, Staffordsire, 1988, pp. 587–592.
24. XUE, L. A. & CHEN, I.-W., Deformation and grain growth of low-temperature-sintered high-purity alumina. *J. Am. Ceram. Soc.*, **73** (1990) 3518–3521.
25. XUE, L. A., WU, X. & CHEN, I.-W., Superplastic alumina ceramics with grain growth inhibitors. *J. Am. Ceram. Soc.*, **74** (1991) 842–845.
26. YOSHIZAWA, Y. & SAKUMA, T., High-temperature deformation and cavitation in fine-grained alumina. *Mater. Sci. Eng.*, **A176** (1994) 447–453.
27. SHIRASUKA, K. & YAMAGUCHI, G., Precise measurement of crystal date and the solid solution range of the defective spinel, $MgO \sim nAl_2O_3$. *Yogyo-Kyokai-Shi*, **82** (1974) 650–653.
28. SAKUMA, T., A novel view on superplasticity in fine-grained caramics. *Mater. Sci. Forum*, **233–234** (1996) 321–332.
29. OKADA, K. & SAKUMA, T., Tensile ductility in zirconia-dispersed alumina at high temperatures. *J. Am. Ceram. Soc.*, **79** (1996) 499–502.
30. LAPPALAINEN, R., PANNILLAT, A. & RAJ, R., Superplastic flow in non-stoichiometric ceramics: Magnesium aluminate spinel. *Acta Metall. Mater.*, **41** (1993) 1229–1235.